

The adipose tissue triglyceride lipase ATGL/PNPLA2 is downregulated by insulin and TNF- α in 3T3-L1 adipocytes and is a target for transactivation by PPAR γ

Ji Young Kim, Kristin Tillison, Jun-Ho Lee, David A. Rearick and Cynthia M. Smas

Am J Physiol Endocrinol Metab 291:E115-E127, 2006. First published 16 May 2006;
doi:10.1152/ajpendo.00317.2005

You might find this additional info useful...

This article cites 81 articles, 51 of which can be accessed free at:

<http://ajpendo.physiology.org/content/291/1/E115.full.html#ref-list-1>

This article has been cited by 20 other HighWire hosted articles, the first 5 are:

Glyceroneogenesis is inhibited through HIV protease inhibitor-induced inflammation in human subcutaneous but not visceral adipose tissue

Stéphanie Leroyer, Camille Vatier, Sarah Kadir, Joëlle Quette, Charles Chapron, Jacqueline Capeau and Bénédicte Antoine

J. Lipid Res., February , 2011; 52 (2): 207-220.

[\[Abstract\]](#) [\[Full Text\]](#) [\[PDF\]](#)

Cloning of avian G(0)/G(1) switch gene 2 genes and developmental and nutritional regulation of G(0)/G(1) switch gene 2 in chicken adipose tissue

S.-A. Oh, Y. Suh, M.-G. Pang and K. Lee

J ANIM SCI, February , 2011; 89 (2): 367-375.

[\[Abstract\]](#) [\[Full Text\]](#) [\[PDF\]](#)

Breed difference and regulation of the porcine Sirtuin 1 by insulin

T. Shan, Y. Ren, Y. Liu, L. Zhu and Y. Wang

J ANIM SCI, December , 2010; 88 (12): 3909-3917.

[\[Abstract\]](#) [\[Full Text\]](#) [\[PDF\]](#)

Triacylglycerol lipases and metabolic control: implications for health and disease

Matthew J. Watt and Lawrence L. Spriet

Am J Physiol Endocrinol Metab, August , 2010; 299 (2): E162-E168.

[\[Abstract\]](#) [\[Full Text\]](#) [\[PDF\]](#)

Mammalian Target of Rapamycin Complex 1 Suppresses Lipolysis, Stimulates Lipogenesis, and Promotes Fat Storage

Partha Chakrabarti, Taylor English, Jun Shi, Cynthia M. Smas and Konstantin V. Kandror

Diabetes, April , 2010; 59 (4): 775-781.

[\[Abstract\]](#) [\[Full Text\]](#) [\[PDF\]](#)

Updated information and services including high resolution figures, can be found at:

<http://ajpendo.physiology.org/content/291/1/E115.full.html>

Additional material and information about *AJP - Endocrinology and Metabolism* can be found at:

<http://www.the-aps.org/publications/ajpendo>

This information is current as of June 3, 2011.

The adipose tissue triglyceride lipase ATGL/PNPLA2 is downregulated by insulin and TNF- α in 3T3-L1 adipocytes and is a target for transactivation by PPAR γ

Ji Young Kim, Kristin Tillison, Jun-Ho Lee, David A. Rearick, and Cynthia M. Smas

Department of Biochemistry and Cancer Biology, Medical University of Ohio, Toledo, Ohio

Submitted 14 July 2005; accepted in final form 30 January 2006

Kim, Ji Young, Kristin Tillison, Jun-Ho Lee, David A. Rearick, and Cynthia M. Smas. The adipose tissue triglyceride lipase ATGL/PNPLA2 is downregulated by insulin and TNF- α in 3T3-L1 adipocytes and is a target for transactivation by PPAR γ . *Am J Physiol Endocrinol Metab* 291: E115–E127, 2006; doi:10.1152/ajpendo.00317.2005.—The minimal adipose phenotype of hormone-sensitive lipase (HSL)-null mice suggested that other hormonally responsive lipase(s) were present in adipocytes. Recent studies have characterized a new adipose tissue triglyceride lipase, ATGL/PNPLA2/destnutrin/iPLA2 ζ /TTS2.2 (ATGL). We had previously cloned a novel adipose-enriched transcript by differential screening and recently determined its identity with murine ATGL. We report here on the regulation of ATGL by TNF- α and insulin in 3T3-L1 adipocytes and identify ATGL as a target for transcriptional activation by the key adipogenic transcription factor PPAR γ . Insulin at 100 nM resulted in a marked decrease in ATGL transcript that was effectively blocked by inhibitors for PI 3-kinase and p70 ribosomal protein S6 kinase. TNF- α treatment decreased ATGL transcript in a time-dependent manner that paralleled TNF- α downregulation of PPAR γ with a maximal decrease noted by 6 h. TNF- α effects on ATGL were attenuated by pretreatment with PD-98059, LY-294002, or rapamycin, suggesting involvement of the p44/42 MAP kinase, PI 3-kinase, and p70 ribosomal protein S6 kinase signals. To study transcriptional regulation of ATGL, we cloned 2,979 bp of the murine ATGL 5'-flanking region. Compared with promoterless pGL2-Basic, the -2979/+21 ATGL luciferase construct demonstrated 120- and 40-fold increases in activity in white and brown adipocytes, respectively. Luciferase reporter activities for a series of eight ATGL promoter deletions revealed that the -928/+21, -1738/+21, -1979/+21, and -2979/+21 constructs were transactivated by PPAR γ . Our findings identify the novel lipase ATGL to be a target gene for TNF- α and insulin action in adipocytes and reveal that it is subject to transcriptional control by PPAR γ -mediated signals.

gene regulation; adipogenesis; promoter activity; tumor necrosis factor- α ; peroxisome proliferator-activated receptor- γ ; patatin-like phospholipase domain containing 2

ADIPOSE TISSUE STORES EXCESS ENERGY INTAKE in the form of triglyceride and mobilizes this storage in the form of free fatty acids (FFAs) to meet the energy demands of the organism. In states of derangement of adipose tissue function such as occur in obesity and type 2 diabetes (50), excessive elevation of plasma FFAs leads to FFA deposition in nonadipose tissues, resulting in a number of detrimental effects, including apoptosis, insulin resistance, fatty acid-induced cellular toxicity, and β -cell dysfunction (71, 72). Adipogenesis is a highly integrated process often depicted as a cascade of gene expression events

initiated by the nuclear hormone transcription factor peroxisome proliferator-activated receptor- γ (PPAR γ) in concert with CCAAT enhancer-binding proteins (52) and sterol regulatory element-binding protein-1/adipocyte determination differentiation-dependent factor 1 (SREBP-1/ADD1) transcription factors (53). FFA metabolites function as ligands for PPAR γ (26, 67, 68), and polyunsaturated fatty acids act to regulate the expression of SREBP-1/ADD1 (23, 69). Given their far-ranging impact in a variety of cell types, understanding the molecular mechanisms underlying the release of FFA from adipose tissue stores is key to the development of appropriate interventions for diabetes, obesity, and related disorders.

Lipolysis in adipocytes is subject to tight regulation by various hormones and cytokines. Until very recently, hormone-sensitive lipase (HSL) was regarded as the only rate-limiting lipolytic activity in adipocytes (58), where its action is subject to tight regulation by catecholamines and insulin (5, 7, 8, 11, 19, 75). Despite much in vitro data supporting a sole and dominant role for HSL in adipocyte triglyceride lipolysis, this notion was not upheld by the phenotype of HSL-null mice (12, 15, 16, 19, 40, 42, 43, 51, 74, 80). HSL-null mice were not obese (12, 16, 74, 80), and their adipose tissues possessed substantial hormone-stimulated triglyceride hydrolysis activities (15, 40, 42, 43, 74), with accumulated diglycerides in white adipose tissue, brown adipose tissue, muscle, and testis (15, 40). That HSL-null mice demonstrated a block in hormone-stimulated glycerol release from adipose tissue led to the conclusion that HSL is a rate-limiting enzyme for the cellular catabolism of diglycerides in adipose tissue and muscle (15, 19, 40) but that other hormone-sensitive non-HSL lipase(s) were responsible for the hydrolysis of triglycerides to diglycerides in adipose tissue (58). Proving this to be the case are three recent reports on the initial identification and characterization of a transcript that is highly restricted to adipose tissue and whose encoded protein functioned as a novel triglyceride lipase (22, 73, 81). The HUGO Committee on Gene Nomenclature and the Mouse Genome Informatics Committee have termed this gene patatin-like phospholipase domain-containing 2, or PNPLA2; however, this gene is variously termed adipose tissue triglyceride lipase (ATGL) (81), desnutrin (73), or iPLA2 ζ (22). For clarity, we refer to it herein solely by the ATGL designation. ATGL is related to plant-derived lipases of the patatin domain protein family (1, 2, 18, 21, 36, 38, 78) and contains a classical lipase signature motif G-X-S-X-G and a α/β -hydrolase fold structure (41, 59). In contrast to HSL,

Address for reprint requests and other correspondence: C. M. Smas, Dept. of Biochemistry and Cancer Biology, Medical University of Ohio, Toledo, OH 43614 (e-mail: csmas@meduohio.edu).

The costs of publication of this article were defrayed in part by the payment of page charges. The article must therefore be hereby marked "advertisement" in accordance with 18 U.S.C. Section 1734 solely to indicate this fact.

which acts on a variety of lipid substrates, including triglycerides, diglycerides, cholesteryl esters, and retinyl esters (reviewed in Ref. 75), ATGL selectively mediates lipolysis of triglycerides (22, 73); it also possesses acylglycerol transacylase activity (22). The catalytic activity of ATGL has recently been demonstrated to involve the serine in the putative Ser-Asp catalytic active site dyad motif (28). Unlike the somewhat broad tissue distribution of HSL, the ATGL transcript shows enriched expression in adipocytes (29, 73, 81), and studies in murine 3T3-L1 adipocytes indicate ATGL functions in basal and isoproterenol-stimulated lipolysis (81). In murine adipose tissue, ATGL transcript level transiently increases during fasting and decreases upon refeeding (73), suggesting that its regulation is closely tied to the metabolic state of the organism. Although the full impact of ATGL on lipolysis and systemic energy balance awaits *in vivo* analysis of gain- and loss-of-function animal models and a thorough assessment in human adipose tissue function, its identification has led to a significant revision of long-held views on triglyceride lipolysis and regulation of fatty acid mobilization from adipose tissue (49, 78). The current working model is one of a two-step process wherein ATGL preferentially hydrolyzes the triglyceride ester bond to generate diglycerides, whereas HSL is primarily responsible for the hydrolysis of diglycerides (78).

In the course of differential screening for adipocyte-specific genes, we identified a transcript whose expression was highly restricted to mature adipocytes and dramatically upregulated during *in vitro* adipogenic conversion of 3T3-L1 preadipocytes. At that time, the human homolog of this gene was in the NCBI GenBank database as an uncharacterized gene of unknown function, termed transport-secretion 2.2 (TTS2.2). During our ongoing analysis of the expression and regulation of murine TTS2.2, it became evident that this novel clone was identical to ATGL. We report herein additional data of the nature of ATGL regulation. We add to the existing data on the differentiation-dependent upregulation of ATGL during adipogenic conversion by use of primary preadipocyte culture models and report that ATGL is a target for downregulation by two factors closely linked to insulin resistance, insulin and TNF- α . Moreover, for the first time, we assess transcriptional regulation of the murine ATGL gene via cloning and analysis of the promoter region and determine that it is a target for transactivation by the key adipogenic transcription factor PPAR γ . We believe these studies of ATGL gene regulation are a key step in furthering our understanding of the role of this novel lipase in adipose tissue and energy balance.

MATERIALS AND METHODS

Adipocyte differentiation and treatments. 3T3-L1 cells (American Type Culture Collection, Manassas, VA) were propagated in Dulbecco's modified Eagle's medium (DMEM) supplemented with 10% calf serum. For differentiation, 3T3-L1 cells were treated at 2 days postconfluence with DMEM supplemented with 10% fetal calf serum (FCS) in the presence of the adipogenic inducers 5 mM methylisobutylxanthine (MIX) and 1 μ M dexamethasone for 48 h. Adipogenic agents were then removed, and growth of cultures continued in DMEM containing 10% FCS. At 5 days postinduction of differentiation, adipocyte conversion had occurred in ~90% of the cells, as judged by lipid accumulation and cell morphology. For studies of regulation by insulin, 3T3-L1 adipocytes were first cultured for 16 h in serum-free and glucose-free DMEM with 0.5% bovine serum albumin (BSA), 1 mM pyruvate, and 1 mM lactate. Cultures were then

replenished with serum-free DMEM containing 0.5% BSA supplemented with insulin (0.2 or 2 μ M) or 4.5 g/l D-glucose, separately or in combination, as indicated, for an additional 6 or 24 h. For treatments of 3T3-L1 adipocytes with TNF- α , cells were incubated with TNF- α for the indicated dose and time points. For treatment with various inhibitors, after serum starvation for 6 h, 3T3-L1 adipocytes were pretreated with either 50 μ M PD-98059, 20 μ M SB-203580, 50 μ M LY-294002, or 1 μ M rapamycin (Sigma-Aldrich, St. Louis, MO) or DMSO vehicle for 1 h and stimulated with 100 nM insulin or 10 ng/ml TNF- α for 16 h in the presence of the indicated inhibitors or incubated with inhibitors only.

For differentiation of brown preadipocytes obtained from C. R. Kahn (Joslin Diabetes Foundation, Harvard Medical School, Boston, MA), cells were cultured to confluence in DMEM with 10% FCS, 20 nM insulin, and 1 nM triiodothyronine [differentiation medium per Kahn et al. (24)]. Confluent cells were incubated in differentiation medium that contained 0.5 mM MIX, 0.5 μ M dexamethasone, and 0.125 mM indomethacin for 24–48 h. Following this period, nearly 100% of cells showed adipogenic conversion, at which time medium was replaced with differentiation medium and was replenished every 2 days.

For culture and differentiation of primary white adipocytes, white adipose tissue collected from male Sprague-Dawley rats was digested with 1 mg/ml type I collagenase for 40 min with shaking at 37°C. Following digestion, material was filtered through a 300- μ m pore size nylon mesh (Sefar America, Depew, NY) and filtrate centrifuged at 2,000 rpm for 5 min. The floating adipocyte fraction was removed, and the pellet of stromal-vascular cells was resuspended in DMEM containing 10% FCS and plated. Upon confluence, cells were either harvested or subjected to differentiation medium consisting of DMEM containing 10% FCS, 0.1 μ M dexamethasone, 0.25 mM MIX, and 17 nM insulin for 3 days, at which time differentiation medium was removed, and cell cultures were maintained in DMEM containing 10% FCS and 17 nM insulin. Human preadipocyte RNA and RNA from *in vitro* differentiated human adipocytes were purchased from Zen-Bio (Research Triangle Park, NC).

RNA preparation, Northern blot analysis, and DNA array hybridization. RNA was purified using TRIzol reagent (Invitrogen) according to manufacturer's instructions. For array analysis, duplicate mouse ResGen GeneFilter Arrays (Invitrogen) containing 5,184 cDNAs were processed exactly per manufacturer's instructions. Filters were hybridized with reverse-transcribed [³²P]cDNA probes synthesized from 8 μ g of total RNA from 3T3-L1 preadipocytes, adipocytes, kidney, brain, or liver. For studies of ATGL expression in murine tissues, 8-wk-old C57BL/6 or *ob/ob* male mice and 8-wk-old SMJ and NZB/BINJ male mice were utilized. In the former case, three adipose tissue RNA samples were found to be degraded and were excluded from further analysis. For Northern blot analysis, 5 μ g of RNA were fractionated in 1% agarose-formaldehyde gels in MOPS buffer and transferred to Hybond-N membrane (GE Healthcare, Piscataway, NJ). As indicated, blots were hybridized in ExpressHyb solution (BD Biosciences Clontech, Palo Alto, CA) with ³²P-labeled specific cDNA probes for murine, human, and rat ATGL, murine adipocyte fatty acid-binding protein (aFABP), murine uncoupling protein-1 (UCP1), and murine PPAR γ . After a washing, the membranes were exposed at -80°C to Kodak Biomax film with a Kodak Biomax intensifying screen. For quantitative assessments, to correct for possible variations in mass of RNA per gel lane, the same blot was hybridized with a probe for 36B4 transcript, which encodes the acidic ribosomal phosphoprotein PO, a commonly employed internal control (27). In these cases, visual assessment of gel loading indicated by ethidium bromide-stained rRNA closely paralleled the 36B4 transcript level. The ratio of expression signal for ATGL transcript to 36B4 transcript for each sample was determined using a Typhoon 8600 PhosphorImager and ImageQuant software (GE Healthcare). Statistical analyses were conducted using single-factor ANOVA.

Animal treatments. For fasting and refeeding studies, 8-wk-old male C57BL/6 mice were subjected to overnight food deprivation. The next morning, animals were refed with a high-carbohydrate, fat-free diet, and tissue was harvested 8 h later. Studies were conducted in duplicate, and an identical regulation pattern of ATGL transcript was observed in fasting and refeeding. All procedures were carried out with approval from the Medical University of Ohio Animal Care and Use Committee. RNA for streptozotocin-treated and insulin-treated mice was a generous gift of H. S. Sul, University of California, Berkeley, CA. Details of these treatments have been published elsewhere (39).

Immunofluorescence localization of ATGL protein in 3T3-L1 adipocytes and preadipocytes. Expression constructs for ATGL were generated by PCR amplification of coding sequences using a murine I.M.A.G.E clone (GenBank no. AI930274) as template. For preparation of an ATGL expression construct, in which a COOH-terminal HA epitope tag was fused to the ATGL coding sequence, a 5' PCR primer (5'-TCACGGTACCGGATCCTTCCCGAGGGAGACCAAGTGG-3') was used in combination with a 3' primer that incorporated a COOH-terminal HA tag followed by a stop codon (5'-CTTAAAGCTTTCAAAGAGCGTAATCTGGAACATCGTATGG GTAGCAAGGCGGGAGGCCAGGTGGATC-3'). In both instances, a 5' *KpnI* site (boldface) and a 3' *HindIII* site (boldface) were incorporated into respective primers to facilitate directional cloning into the pQETri vector (Qiagen, Valencia, CA). 3T3-L1 preadipocytes or differentiated 3T3-L1 adipocytes were plated onto laminin-coated coverslips and transfected with either HA-tagged ATGL expression construct or empty pQETri vector using Lipofectamine 2000 (Invitrogen). At 24 to 48 h posttransfection, cells were fixed and permeabilized. After blocking with 0.1% BSA for 30 min, rabbit polyclonal antibody against the HA epitope tag (1:100 dilution; Santa Cruz Biotechnology, Santa Cruz, CA) was used as primary antibody. Fluorescein isothiocyanate (FITC)-conjugated goat anti-rabbit IgG (Sigma-Aldrich) secondary antibody was utilized at a 1:100 dilution. For visualization of lipid droplets, lipid was stained by incubation of immunostained cells with 0.5 μ g/ml Nile red (Molecular Probes, Eugene, OR). Negative controls included staining with non-related primary antibody, staining of transfected cells with secondary antibody only, and vector-only transfectants. After processing, coverslips were mounted on glass slides and viewed with a Nikon Eclipse E800 fluorescence microscope equipped with a digital camera. Image acquisition and merging was performed with Image-Pro Plus software (Media Cybernetics, Carlsbad, CA).

Luciferase analysis of ATGL promoter activity. To prepare luciferase reporter constructs containing ATGL promoter regions, phage DNA for murine ATGL genomic clones was subjected to 12 cycles of PCR with primers designed based on murine ATGL genomic flanking region sequence available through the murine Ensembl database (www.ensembl.org). PCR was conducted with a promoter proximal primer (5'-GCGAAAGCTTCGGCGGAGGCGGAGACGCTGTGC-3') spanning through (+)21 of the ATGL transcript in combination with the promoter-distal primer for the -192/+21 promoter construct (5'-GCCGCTAGCGGAGCCACAGGATCAGGCAGC-3'), for the -606/+21 promoter construct (5'-GCCGCTAGCGCTGAAGCCTGGGAATCCCCTCTC-3'), for the -795/+21 bp promoter construct (5'-gcgggctagcaccataaaccaacctgtttg-3'), for -1979/+21 bp promoter construct (5'-gacggctagctaggacccggctctcttttcag-3'), or for -2979/+21 bp promoter construct (5'-GACGGCTAGCACAGCAGGAGAAGAAAGA-3'). Primer sequence included a 5' *NheI* site (boldface) and a 3' *HindIII* site (boldface), and the resulting PCR products were ligated into the corresponding restriction sites of pGL2-Basic vector (Promega, Madison, WI). The -1738/+21, -928/+21, and -373/+21 promoter constructs were generated by cutting the -1979/+21 construct with *SacI*, *SmaI*, or *KpnI*, respectively, to remove a portion of the 5' region, followed by ligation. Promoter constructs were confirmed by restriction digest and complete sequencing.

For transfection studies on expression of the ATGL promoter in adipocytes, we utilized the 3T3-L1 cell line and a brown preadipocyte cell line. Both cell lines were treated with differentiation agents for 48 h, as described above. The following day, cells were trypsinized and replated at 3.4×10^4 cells/cm² and transfected the next day using Lipofectamine 2000. For transfection studies to assess transcriptional activation of the murine ATGL promoter by PPAR γ transcriptional signals, each of the ATGL promoter-luciferase constructs was transfected into HeLa cells. As indicated, these transfections also included murine PPAR γ and murine retinoid X receptor- α (RXR α) expression constructs, a generous gift from R. Evans, The Salk Institute for Biological Studies, La Jolla, CA. A PPAR γ -responsive promoter construct, 3XPPRE-Luc, also provided by R. Evans, was utilized as a positive control to determine that transcriptional activation by the transfected the PPAR γ /RXR α constructs was functional in our hands. At 24 or 48 h posttransfection, cells were treated with 10 μ M 15-deoxy- $\Delta^{12,14}$ -prostaglandin J₂ (Caymen Chemical, Ann Arbor, MI), a PPAR γ ligand, for 24 h. Firefly and *Renilla* luciferase activities were determined at 48 or 72 h posttransfection using the Dual Luciferase Reporter Assay System and a Turner Industries luminometer (Promega). Statistical analyses were conducted using single factor ANOVA.

RESULTS AND DISCUSSION

Identification of murine ATGL as a differentially regulated gene in multiple models of white and brown adipogenesis. To identify and characterize new genes that may be important in adipocyte function, we undertook DNA array analysis of 5,184 cDNA inserts utilizing murine GeneFilters Arrays. Differential screening was conducted via hybridization with reverse-transcribed probes prepared from 3T3-L1 preadipocyte or 3T3-L1 adipocyte total RNA. Subsequent rounds of filter hybridization with reverse-transcribed probes from kidney, brain, and liver were performed (data not shown), and we focused our study on one clone that appeared to be adipocyte enriched. The differential signal for this clone is shown in Fig. 1A. We conducted RT-PCR-based cloning and 5' RACE and 3' RACE analysis on total RNA from white and brown adipose tissue and cloned and sequenced the full-length murine cDNA consisting of 1,961 nucleotides with a 486-amino acid open-reading frame. Database analyses revealed that this gene was the murine homolog of a human gene termed TTS2.2, whose function was not previously known. We submitted this sequence to GenBank under the designation murine TTS2.2, accession no. AY510273. Recent studies by three independent research groups have reported on the initial identification of a novel adipose tissue-expressed gene and characterized its triglyceride lipase activity. This novel gene was TTS2.2, which has been renamed adipose triglyceride lipase (ATGL) (81), destnutrin (73), or calcium-independent phospholipase iPLA₂ ζ (22).

To assess the expression pattern of ATGL during adipogenic conversion, we conducted Northern blot analysis using various models representing both white and brown adipocyte differentiation. The recently published findings on ATGL indicated that it was dramatically increased upon in vitro white adipose conversion of the 3T3-L1 cell line (22, 73, 81), as we also found (Fig. 1B). We have extended the differentiation-dependent upregulation of ATGL to other important models of adipogenesis, including assessment of adipogenic conversion of primary cells. This is particularly important as significant differences between gene expression profiles for in vitro and in

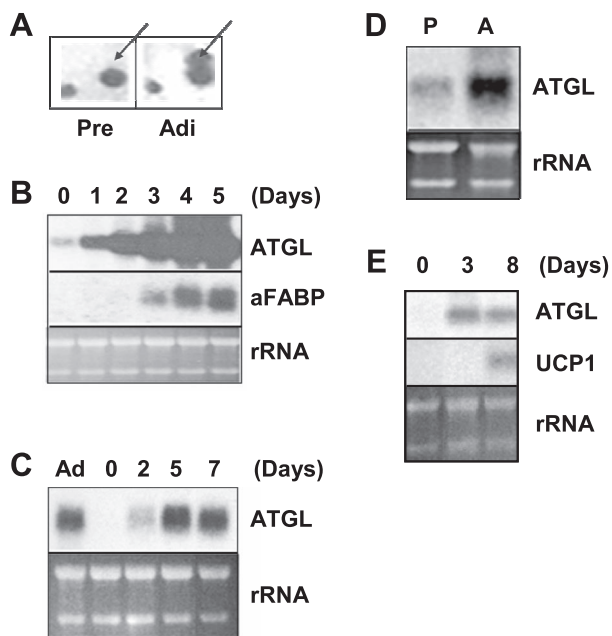


Fig. 1. Upregulation of adipose tissue triglyceride lipase (ATGL) transcript is common to multiple models of adipogenesis. *A*: initial filter array hybridization of ATGL as a novel gene upregulated in 3T3-L1 adipogenesis. Shown is the portion of the DNA filter array indicating the specific ATGL signal (arrow) in 3T3-L1 adipocytes (Adi) and lack of signal in 3T3-L1 preadipocytes (Pre). *B*: ATGL upregulation during 3T3-L1 differentiation. 3T3-L1 cells were harvested before induction of adipogenesis (*day 0*) and indicated time points. Northern blot analysis was performed with ATGL and adipose fatty acid-binding protein (aFABP) cDNA probes. *C*: ATGL upregulation in rat primary preadipocyte differentiation. Stromal-vascular fraction cells from rat white adipose tissue (WAT) were harvested and cultured in DMEM containing 10% FCS. Confluent cells were subjected to induction of adipogenic differentiation with dexamethasone, methylisobutylxanthine (MIX), and insulin. RNA was prepared at confluence (*day 0*) and at 2, 5, and 7 days postinduction and hybridized with a rat partial ATGL cDNA probe. Murine adipose tissue total RNA (Ad) was included as a positive hybridization control. *D*: ATGL in human adipogenesis. Preadipocytes (P) were from human adipose tissue and adipocytes (A) from *in vitro* differentiation of human preadipocytes and analyzed by Northern blot using a human ATGL cDNA probe. *E*: ATGL transcript expression in brown adipogenesis. Brown preadipocytes were differentiated as described in MATERIALS AND METHODS at confluence (*day 0*). Brown adipocytes were harvested at 3 and 8 days, and Northern blot analysis was performed with murine ATGL and uncoupling protein-1 (UCP1) probes. For *B–E*, ethidium bromide (EtBr) staining of rRNA is shown as gel-loading control.

vivo adipogenesis exist (62). Figure 1C illustrates that the ATGL message was not detected in the preadipocyte-containing stromal-vascular fraction of rat adipose tissue but was dramatically induced upon their adipogenic differentiation. ATGL has been detected in human adipose tissue biopsy (81), and we show herein that upregulation of ATGL transcript occurs during *in vitro* differentiation of human primary preadipocytes to adipocytes (Fig. 1D). The regulation of ATGL in brown adipogenic conversion had not previously been addressed. We therefore determined whether *in vitro* brown adipogenesis is accompanied by emergence of ATGL transcript. Figure 1E demonstrates that the ATGL transcript was not found in brown preadipocytes but was present by 3 days postinduction of differentiation, and a similar level of ATGL transcript is present at *day 8*. The brown adipocyte-specific transcript UCP1 expression at *day 8* indicates mature brown adipocytes.

Expression of ATGL is widespread, with adipose tissue the dominant site. We have examined ATGL transcript level in a wide assortment of murine tissues and find that, as previously indicated (73, 81), adipose tissue is clearly the dominant site of ATGL transcript expression (Fig. 2A), where it is present at a level similar to that found in 3T3-L1 adipocytes. Compared with robust expression in adipose tissue, ATGL transcript is detected at an approximately fivefold lower level in testis and at readily detectable albeit markedly lower levels in all other tissues examined. As has been reported in the literature (73), we also find ATGL transcript to be present in the adipocyte component and not in the stromal-vascular component of white adipose tissue (data not shown). We next determined whether expression of ATGL transcript is dysregulated in obesity by using the leptin deficient *ob/ob* mouse model. Studies by Villena et al. (73) reported that, following a 12-h fast, the level of ATGL transcript was dramatically lower in *ob/ob* or *db/db* mice compared with that in wild-type mice. Whether the level of ATGL is altered in genetically obese mice under ad libitum conditions was not noted. We compared the level of ATGL transcript expressed under ad libitum conditions by wild-type or *ob/ob* mice in subcutaneous and epididymal white adipose depots, liver, and kidney. The data for the Northern blot analysis are presented in Fig. 2B. We found that the level of ATGL transcript was significantly lower in *ob/ob* subcutaneous and epididymal white adipose depots, with a mean decrease to 47% ($P < 0.001$) and 61% ($P < 0.05$), respectively, of wild-type values. Our findings support the notion that, when adipose tissue becomes insulin resistant, as would occur in conditions of obesity, the fall in plasma insulin concentration during fasting may not trigger lipolysis and FFA release from adipose tissue to the same degree as in the nonobese state (56). As is evident in the data for the epididymal depot, we observed that the level of ATGL transcript varies considerably in individual animals in this white adipose depot; in contrast we found a high degree of consistency in the ATGL level in the subcutaneous depot. We also find a moderate (17%) but statistically significant ($P < 0.005$) increase in the ATGL transcript level in liver of *ob/ob* mice. This may reflect the general dysregulation of adipose tissue function that accompanies obesity, wherein nonadipose organs often adopt metabolic and gene expression characteristics of mature fat cells (33, 71). The level of ATGL transcript in kidney did not differ for wild-type vs. *ob/ob* mice ($P > 0.05$). It should be noted that our finding of alterations of ATGL transcript in *ob/ob* adipose tissues and liver differs from that recently reported by Lake et al. (28), while this paper was under revision. Lake et al. assessed the level of ATGL transcript in 10-wk-old wild-type and *ob/ob* mice under ad libitum conditions using TaqMan real-time quantitative RT-PCR and failed to find statistically significant differences ($P > 0.05$) in liver or adipose tissue, although the specific white adipose tissue depot they examined was not stated. Although the underlying basis for these differing observations cannot be known at this time, our findings on downregulation of ATGL in *ob/ob* adipose tissues appear to be in line with those of Villena et al., although in the latter case fasted animals were utilized (73). To further examine ATGL transcript levels in relation to body weight and adiposity, we assessed two inbred strains of mice, SM/J and NZB/BINJ; SM/J mice are genetically lean compared with NZB/BINJ (31, 48). Here, we find a rather wide degree of animal-to-animal

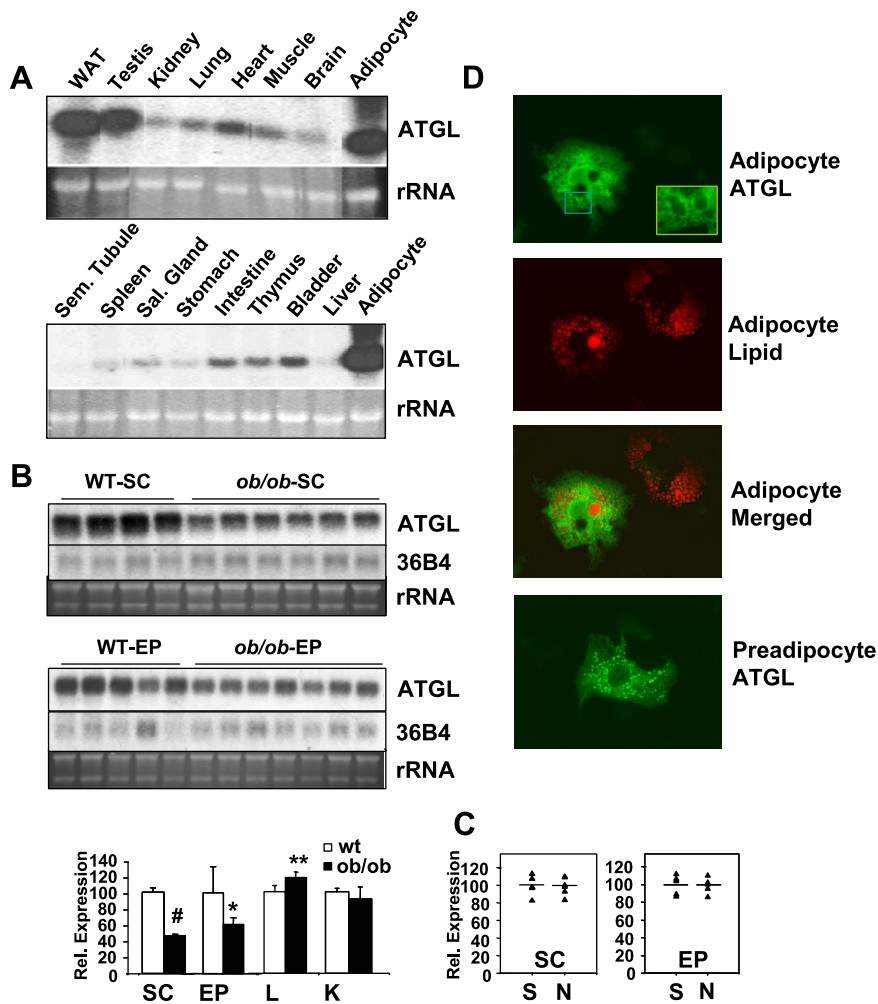


Fig. 2. Expression pattern of ATGL transcript and localization of ATGL protein. **A**: ATGL transcript level in a panel of murine tissues. Total RNA (5 μ g) from indicated mouse tissues were analyzed by Northern blot using murine ATGL cDNA probe. 3T3-L1 adipocyte RNA was loaded for positive control (Adipocyte). EtBr staining of rRNA was used as gel-loading control. **B**: expression of ATGL transcript in tissues of wild-type (wt) and obese (*ob/ob*) mice. Subcutaneous (SC) and epididymal adipose tissue (EP), liver (L), and kidney (K) RNA was isolated from 8-wk-old wt C57BL/6 and *ob/ob* mice and subjected to Northern blot hybridization for ATGL and 36B4 levels, quantitated by Phosphor-Imager analysis, and ATGL transcript level for each sample normalized against its 36B4 control to correct for possible variations in sample loading. Data represent normalized ATGL means \pm SD from wt mice ($n = 4$ for SC, $n = 5$ for EP, $n = 6$ for liver and kidney) or *ob/ob* mice ($n = 6$ for SC, $n = 7$ for EP, liver, kidney) and were analyzed by single-factor ANOVA ($*P < 0.05$, $**P < 0.005$, $\#P < 0.001$). **C**: ATGL expression in WAT of mouse strains. EP and SC adipose tissue RNA was harvested from SM/J (S, $n = 5$) and NZB/BINJ (N, $n = 6$) male mice and analyzed as described in **B**. Individual animals are represented by triangles, with horizontal line indicating group mean, which was not significantly different between groups ($P > 0.05$). **D**: localization of ATGL protein in adipocytes. 3T3-L1 adipocytes were transfected with HA-tagged ATGL expression construct and then fixed and stained with anti-HA antibody followed by FITC-conjugated goat anti-rabbit IgG as described in MATERIALS AND METHODS. Images showed HA-tagged ATGL in green (*top*), lipid in red after Nile red staining (*upper middle*), and merged image in 3T3-L1 adipocytes (*lower middle*). ATGL expression in 3T3-L1 preadipocytes is also shown (*bottom*).

variation of ATGL transcript level under ad libitum conditions within the two strains but fail to find a statistically significant alteration in ATGL transcript level between NZB/BINJ and SM/J mice (Fig. 2C, right). It is likely that investigation of other models of animal obesity, as well as that of human obesity, will shed additional light on the alteration in ATGL transcript level in adipose and other tissues in obese states.

Immunostaining analyses in 3T3-L1 preadipocytes and adipocytes suggests that intracellular lipid impacts ATGL protein distribution pattern. Before the recent demonstration by several groups that ATGL acts as a lipase (22, 73, 81), a few reports had suggested that localization of ATGL protein was closely associated with lipid droplet formation and/or function. Proteomic analysis of lipid droplets in CHO-K2 cells, a cell type that spontaneously accumulates lipid droplets upon confluence, indicated that the adipocyte lipid droplet is likely a highly dynamic metabolic organelle that is directly involved in membrane traffic, termed "adiposome". One of the ~ 40 proteins found in this proteomic analysis was encoded by a murine expressed sequence tag (EST) corresponding to ATGL (34). A second study, in lipid-loaded A431 cells, identified ATGL as a component of their lipid droplet proteome (70). These observations imply that the expression of ATGL protein correlates closely with the ability of a cell to process and/or turn over triglyceride stores whether or not the cell type actually is an

"adipocyte". Herein, we show, using immunostaining for HA-tagged ATGL protein, that ATGL colocalizes with lipid droplets in 3T3-L1 adipocytes. Figure 2D shows the FITC-linked detection of HA-tagged ATGL (*top*), the staining of intracellular lipid droplets with Nile red (*upper middle*), and the merged image (*lower middle*). ATGL protein is particularly enriched at the surface of intracellular lipid droplets, although signal is also present in other regions of the cytoplasm. Transfection and detection of ATGL in 3T3-L1 preadipocytes, which by definition lack intracellular lipid, revealed a precise punctate signal (*bottom*). This staining pattern may be explained by the possibility that the correct intracellular localization of ATGL protein requires the presence of either lipid droplets and/or other protein components that are present in the mature adipocyte but lacking in the preadipocyte. Our findings on the colocalization of ATGL with lipid droplets in adipocytes by immunostaining agrees with that previously reported using enhanced green fluorescent protein fusion studies in 3T3-L1 adipocytes (81). Although this photomicrographic analysis in adipocytes indicates that ATGL protein is closely associated with adipocyte lipid droplets, subcellular fractionation and Western blot analyses of ectopically expressed epitope-tagged ATGL in either COS cells (73, 81) or 3T3-L1 adipocytes (81) indicate that a substantial fraction of ATGL protein might be cytoplasmic. It is important to keep in mind that, although the

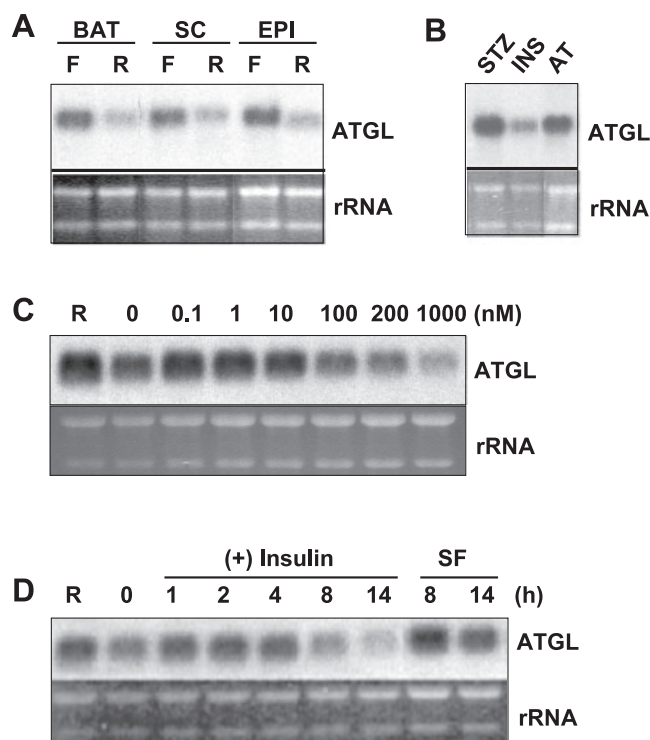


Fig. 3. Nutritional signals and insulin regulate ATGL transcript levels in vivo and in 3T3-L1 adipocytes. *A*: ATGL expression during fasting and refeeding. Mice were fasted overnight and refed a high-carbohydrate diet. After 8 h, brown adipose tissue (BAT) and SC and EP WAT were collected, and total RNA was subjected to Northern blot analysis for ATGL. *B*: insulin regulation of ATGL transcript in vivo. Total RNA from WAT of mice treated with streptozotocin (STZ) or from STZ-treated mice injected with insulin (INS) was used for Northern blot analysis for ATGL. Insulin-mediated downregulation of ATGL is dose dependent in 3T3-L1 adipocytes (*C*) and time dependent (*D*) in 3T3-L1 adipocytes. Differentiated 3T3-L1 adipocytes were incubated in serum-free medium for 16 h (*time 0*) or in regular growth medium (R), at which time serum-free cultures were further incubated with either the indicated concentration of insulin for 36 h (*C*) or 100 nM insulin for the indicated times (*D*). For *A–D*, EtBr staining of rRNA was used as gel-loading control.

existing data support the close association of ATGL protein with adipocyte lipid droplets, the localization or expression studies to date have not examined endogenous ATGL protein. It may also be worth noting that, although two proteomic analyses of lipid-loaded nonadipocyte cell types indicated ATGL protein to be a component of their lipid droplets (34, 70), a study on the proteome of 3T3-L1 adipocyte lipid droplets failed to find ATGL protein in either basal or lipolytically stimulated conditions, whereas HSL was identified under both conditions (6). This may be due merely to technical issues or might reflect the innate character of the endogenous ATGL protein in 3T3-L1 adipocytes. For example, the association of ATGL and lipid droplets may be of a weak and/or highly transient nature or limited to specific physiological conditions. It is well established that HSL undergoes translocation from the cytoplasm to lipid droplets upon stimulation with isoproterenol (7, 8, 11). Studies reported in HSL-null mice indicated that the non-HSL lipase activity in these animals or cells thereof might be subject to isoproterenol stimulated intracellular redistribution from cytosol to fat cake (42). When ATGL was specifically assessed in this regard by Western analysis of ectopically expressed His-tagged ATGL, isoproterenol-stimu-

lated lipolysis did not affect the amount of lipid droplet-associated ATGL (81). However, this does not rule out intracellular redistribution of ATGL protein in response to other stimuli, for example, during TNF- α -induced adipocyte lipolysis.

ATGL transcript is a target of negative regulation by insulin in 3T3-L1 adipocytes. Because defective fatty acid mobilization is one of the key metabolic alterations that occur in type 2 diabetes and ATGL function impacts this mobilization, we assessed regulation of ATGL transcript level by two agents tied to the development of insulin resistance, TNF- α and insulin. Studies we conducted, shown in Fig. 3, *A* and *B*, and those of others (73), reveal that the level of ATGL transcript decreases during the refeeding period of a fasting-refeeding regimen. That this downregulation of ATGL transcript occurs upon insulin administration to streptozotocin-diabetic mice indicates that insulin is a key mediator of ATGL gene expression. As insulin is the key lipogenic hormone, it follows that a lipase would be a likely target for negative regulation by insulin. To precisely address the ability of insulin to regulate ATGL transcript, we utilized in vitro studies with 3T3-L1 adipocytes. Figure 3*C* shows the level of ATGL transcript in response to a 36-h treatment with concentrations of insulin through 1 μ M, revealing a dose-response effect with a decline first observed at 100 nM. We next assessed the temporal nature of insulin-mediated downregulation of the ATGL transcript. Northern blot analysis was conducted on cultures of insulin-treated 3T3-L1 adipocytes harvested at the time points indicated in Fig. 3*D*. Addition of insulin to serum-free cultures of 3T3-L1 adipocytes results in a marked decrease in the level of ATGL transcript at the first time point assessed, 8 h, with a similar decrease at 14 h. No decrease in ATGL transcript was found in time-matched serum free cultures.

We next examined the mode of insulin action in downregulation of ATGL transcript by using inhibitors for specific signaling intermediates. For these studies, 3T3-L1 adipocytes were tested under serum-free conditions by pretreatment with DMSO (vehicle), PD-98059, SB-203580, LY-294002, or rapamycin and were then subjected to insulin treatment. As shown

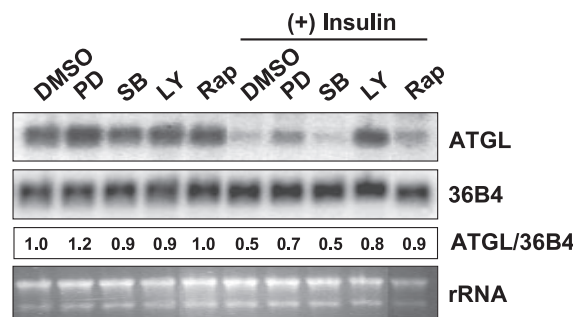


Fig. 4. Role of PI 3-kinase in insulin-mediated ATGL downregulation in 3T3-L1 adipocytes. 3T3-L1 adipocytes were serum starved for 6 h and pretreated for 1 h with DMSO vehicle, PD-98059 (PD, 50 μ M), SB-203580 (SB, 20 μ M), LY-294002 (LY, 50 μ M), and rapamycin (Rap, 1 μ M), at which time they were subjected to continued incubation under these conditions with or without 100 nM insulin for an additional 16 h. Total RNA (5 μ g) was analyzed by Northern blot using ATGL probe. Normalized ATGL expression level was quantitated as described for Fig. 2. Nos. indicate increase or decrease in normalized mean signal, relative to DMSO, which was set to a value of 1.0. Two independently conducted experiments yielded essentially the same results.

by the Northern blot analysis in Fig. 4, the decrease of ATGL transcript by insulin occurred in the presence of DMSO and was not affected by pretreatment with SB-203580, a p38 MAP kinase pathway inhibitor. A partial attenuation of the insulin-mediated downregulation of ATGL was noted with the p44/42 MAP kinase inhibitor PD-98059, whereas the inhibitor of PI 3-kinase LY-294002 and the p70 S6 kinase inhibitor rapamycin showed a nearly complete attenuation of the effects of insulin. This indicates that the PI 3-kinase and p70 S6 kinase pathways are major effectors of insulin downregulation of the ATGL transcript. Because p70 S6 kinase is a target of PKB/Akt-mediated signals, which is in turn a major target of PI 3-kinase, our findings indicate that insulin-mediated ATGL downregulation is mediated via PI 3-kinase and p70 S6 kinase pathways. It should be noted that, during revision of this paper Kralisch et al. (25), using quantitative real-time PCR, also reported that insulin downregulates ATGL transcript in 3T3-L1 adipocytes and that PD-98059 partially rescued the insulin-mediated decrease. However, they reported that LY-294002 was unable to block the effects of insulin on downregulation of ATGL transcript but nonetheless speculated that their lack of statistically significant findings might be attributable to the degree of experimental variation that they observed. One possible explanation for the difference in response to LY-294002 was that our studies utilized 50 μM vs. the 10 μM utilized by Kralisch et al., and we have found that, compared with 50 μM , attenuation of the insulin response at 10 μM LY-294002 is relatively minor (data not shown).

Last, we examined the combined effects of insulin and glucose on ATGL transcript level (Fig. 5). Mature 3T3-L1 adipocytes were subjected to a serum-free, glucose-free medium containing pyruvate, lactate, and BSA for 16 h. Cultures were then supplemented with D-glucose under high (2 μM) or low (0.2 μM) insulin concentrations either singly or in combination. As shown in Fig. 5, a 6-h challenge with the indicated agents did not appreciably affect ATGL transcript levels. At 24 h, a marked decrease is noted with insulin or insulin and glucose in combination. Glucose alone had no effects on ATGL transcript level. This indicates that downregulation of ATGL transcript by insulin is independent of glucose presence in the culture medium. It is known that insulin treatment does

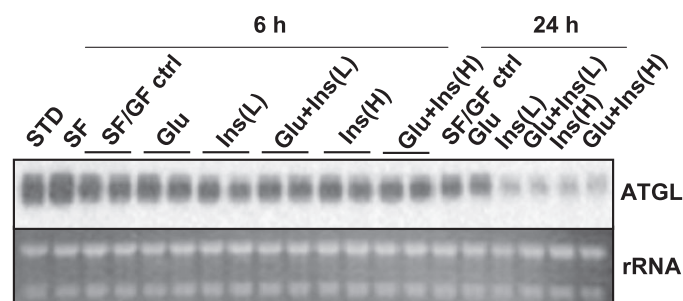


Fig. 5. Insulin downregulation of ATGL transcript in 3T3-L1 adipocytes does not require glucose. 3T3-L1 adipocytes cultured for 16 h in serum-free (SF) and glucose-free (GF) DMEM with 0.5% BSA, pyruvate, and lactate were incubated for an additional 6 h or 24 h in serum-free DMEM with indicated supplements: 4.5 g/l D-glucose (Glu), 0.2 μM insulin [Ins(L)], 2 μM insulin [Ins(H)], or combinations of glucose and insulin as shown (Glu+Ins). 3T3-L1 adipocytes with standard serum- and glucose-containing culture conditions (STD) are also shown. Total RNA (5 μg) was analyzed by Northern blot using ATGL probe. EtBr staining of rRNA was used as gel-loading control.

not appear to affect HSL transcript level in in vitro differentiated 3T3-F442A adipocytes (46), whereas glucose decreases HSL transcript level (60). Thus, in contrast to HSL, ATGL is not regulated by glucose but by insulin per se. Little is known of the other hormones or factors that may regulate ATGL transcript in adipocytes. The only previously reported regulation of ATGL transcript in adipocytes was a moderate increase upon exposure of 3T3-L1 adipocytes to the synthetic glucocorticoid dexamethasone and the marked upregulation of ATGL transcript by dexamethasone in 3T3-L1 preadipocytes (73).

Rapid downregulation of ATGL transcript reveals ATGL to be an early target for TNF- α effects in adipocytes. The cytokine TNF- α has wide-ranging effects on adipose tissue and has been implicated in obesity, insulin resistance, and impaired glucose tolerance (20). TNF- α stimulates lipolysis in adipose tissue, and the subsequent increase in plasma FFAs is a contributing factor in the development of insulin resistance. Because TNF- α is secreted from adipocytes, it is thought to provide a key molecular link between obesity and a chronic inflammatory state that ultimately leads to pathophysiology of adipose tissue and concomitant detrimental systemic effects. Although much about the mechanisms for the lipolytic effects of TNF- α remains to be elucidated, recent data suggest that the extracellular signal-related kinase pathway impacts TNF- α -stimulated lipolysis (64). Other key actions of TNF- α in regard to FFA release are inhibition of insulin signaling (44), inhibition of lipoprotein lipase activity (13), and downregulation of lipoprotein lipase transcript level (9, 77). TNF- α also decreases transcript level for perilipin (54), a protein that mediates the accessibility of lipid droplet triglycerides to lipolysis by HSL (63, 66). TNF- α treatment of mature fat cells results not only in lipolysis per se but in a comprehensive alteration of the adipocyte gene expression profile wherein cells undergo what has been termed "adipocyte dedifferentiation" and take on preadipocyte characteristics (55, 79). Activation of preadipocyte gene expression and suppression of key adipocyte genes, for example the master transcriptional regulator of adipocyte phenotype PPAR γ (55, 79), underlie these effects, with TNF- α -mediated downregulation of PPAR γ resulting in decreased expression of PPAR γ transcriptional targets.

To determine whether ATGL gene expression is regulated by TNF- α , we conducted dose- and time-response studies in mature 3T3-L1 adipocytes. Northern blot analysis data that we present in Fig. 6A demonstrate a negative regulation of ATGL transcript in adipocytes by TNF- α . Treatment of 3T3-L1 adipocytes for 24 h with 0.01 to 100 ng/ml TNF- α results in a marked decrease in ATGL transcript level at TNF- α concentrations of 1 ng/ml and higher. To investigate downstream signals that are involved in TNF- α -mediated downregulation of ATGL transcript, 3T3-L1 adipocytes were pretreated with inhibitors of key signaling cascades prior to the addition of TNF- α . As shown in Fig. 6B, PD-98059, LY-294002, and rapamycin each attenuated the TNF- α -mediated downregulation of ATGL transcript level, whereas no effect was noted with SB-203580. These observations indicate that both PI 3-kinase signals and p44/42 MAP kinase signals are effectors of TNF- α action in this setting. However, SB-203580, a specific inhibitor of the p38 MAP kinase pathway, did not block this downregulation. Recent studies by Kralisch et al. (25), reported during revision of this paper, found that although ATGL was a target for negative regulation by TNF- α in

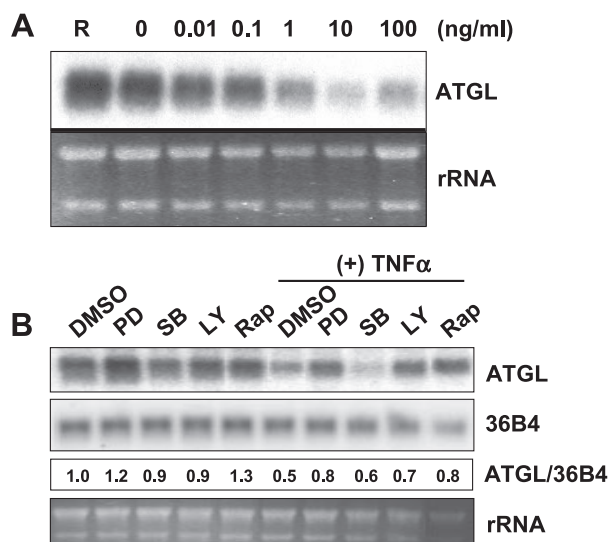


Fig. 6. Adipocyte ATGL transcript is a target for rapid negative downregulation by TNF- α via p42/44 MAP kinase and PI 3-kinase pathways. **A:** 3T3-L1 adipocytes were treated with indicated dose of TNF- α for 24 h, and ATGL expression was analyzed by Northern blot. **B:** 3T3-L1 adipocytes were pre-treated for 1 h with DMSO, PD-98059 (PD, 50 μ M), SB-203580 (SB, 20 μ M), LY-294002 (LY, 50 μ M), and rapamycin (Rap, 1 μ M) before addition of 10 ng/ml TNF- α for 16 h or without TNF- α , and RNA was analyzed for ATGL by Northern blot and quantitated by PhosphorImager analysis. Normalized ATGL expression level was quantitated as described for Fig. 2. Nos. indicate increase or decrease in normalized mean signal relative to DMSO, which was set to a value of 1.0. Two independently conducted experiments yielded essentially the same results.

3T3-L1 adipocytes, no effects of either PD-98059 or LY-294002 were noted. These differing observations may be attributable to their use of a higher concentration of TNF- α than we employed, or other variations in experimental conditions that are not clear at this time.

Although we show that the ATGL transcript is a target for downregulation by TNF- α , it is presently not known whether TNF- α -stimulated lipolysis has effects on ATGL protein function or localization. However, data in HSL-null MEF adipocytes led to the hypothesis that non-HSL intracellular triglyceride lipase(s) may be a key enzyme(s) through which TNF- α stimulates lipolysis (42). At first glance, it would appear that downregulation of ATGL transcript level by TNF- α would counter the ability of TNF- α to most effectively promote lipolysis. It is also fully possible that, although the ATGL transcript is rapidly decreased by TNF- α , the protein level for ATGL would be sustained for a considerably longer period and thus participates in TNF- α -mediated lipolysis. We believe that the transcriptional downregulation of ATGL likely reflects the widespread reduction in expression of adipocyte specific genes, regardless of their functional class, that occurs upon TNF- α treatment of adipocytes. For example, TNF- α treatment of adipocytes not only results in a downregulation of HSL transcript but also downregulates lipoprotein lipase transcript, two genes important for lipolysis and lipogenesis, respectively (55, 57). Thus, although recent transcriptome profiling studies indicate that TNF- α leads to marked and rapid alterations in adipocyte gene expression, the sum of which on balance favors FFA release, there are clearly individual genes whose regulation by TNF- α does not follow this paradigm.

One mechanism of TNF- α in mediating adipocyte dedifferentiation and concomitant loss of intracellular lipid is via its downregulation of PPAR γ expression, which in turn leads to a decreased expression of genes transactivated by PPAR γ (57). We reasoned that, if this was the case for ATGL, then a similar temporal decline in PPAR γ and ATGL transcript might be noted upon TNF- α treatment of 3T3-L1 adipocytes. To investigate the temporal relationship between the effects of TNF- α on PPAR γ and ATGL transcript, we treated 3T3-L1 adipocytes with 10 ng/ml TNF- α for times ranging from 1 through 48 h. Northern blot analysis shown in Fig. 7 indicates that a reduction of ATGL transcript occurs within 6 h of exposure to TNF- α . This closely parallels the reduction of PPAR γ transcript upon TNF- α exposure and supports the notion that ATGL might be a novel PPAR γ target gene. This possibility is further bolstered by a report of Reddy's group [Yu et al. (76)] on the liver gene expression profiles of PPAR γ -null mice that ectopically expressed PPAR γ 1 via adenoviral-driven expression. These mice manifested adipogenic hepatic steatosis, which was accompanied by increased expression of a number of key adipocyte genes in liver. Among these genes was ATGL, wherein a sevenfold increase of the transcript was reported, suggesting the possibility that ectopic expression of PPAR γ might directly activate the ATGL gene promoter.

Functional analysis of the ATGL promoter region identifies ATGL as a novel transcriptional target for PPAR γ -mediated transactivation. Because ATGL has only very recently been identified, much about the in vivo role of ATGL in lipid metabolism awaits the generation and analysis of appropriate murine transgenic and knockout models. However, ATGL is already emerging as a key player in the regulation of adipocyte lipid metabolism, and much remains to be learned of the regulation of this lipase at the protein and gene level. Therefore, studies on the transcriptional control of the 5'-flanking regulatory region of ATGL, for which no information exists to date, are particularly timely and compelling. To begin studies of ATGL transcriptional regulation, we carried out 5' RACE analysis, and the resultant RACE products were sequenced to map the 5' transcriptional start site of the ATGL gene. PCR amplification was used with the phage clone DNA for the ATGL gene as template to amplify a 3,000-bp fragment of the ATGL 5'-flanking region. After full sequencing confirmation of this fragment, it was inserted upstream of a luciferase reporter gene in the pGL2-Basic vector. The resulting -2979/+21LUC construct contained -2979 of the ATGL 5'-flanking region through +21 of the ATGL transcript. We first deter-

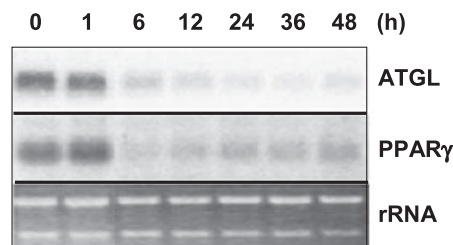


Fig. 7. TNF- α -mediated temporal downregulation of ATGL and PPAR γ transcript in 3T3-L1 adipocytes. 3T3-L1 adipocytes were treated with 10 ng/ml TNF- α for indicated time points. Total RNA (5 μ g) was analyzed by Northern blot using murine ATGL and PPAR γ probes. EtBr staining of rRNA was used as gel-loading control.

mined that this portion of the ATGL promoter was sufficient to drive transcriptional activity in white and brown adipocytes. Transient transfection and luciferase reporter assays of the $-2979/+21$ LUC construct or the empty promoterless pGL2-Basic vector indicated that, compared with the empty vector, $-2979/+21$ LUC resulted in a 240-fold and a 47-fold increase in white and brown adipocytes, respectively (Fig. 8).

To assess the ability of PPAR γ to transactivate the ATGL gene, we generated a set of eight luciferase reporter constructs representing a series of 5' deletions of the ATGL 5' regulatory region, shown in Fig. 9. These were utilized in transient transfection assays wherein they were cotransfected with PPAR γ and its obligate heterodimerization partner RXR α , and cell lysates were assayed at either 48 or 72 h posttransfection. As is shown in Fig. 9, compared with luciferase activities in the absence of PPAR γ /RXR α cotransfection, no significant increase in luciferase reporter gene activity was found upon cotransfection of PPAR γ /RXR α for pGL2-Basic, $-192/+21$, $-373/+21$, $-606/+21$, or $-795/+21$ ATGL promoter constructs. However, the constructs containing additional 5' regions of ATGL promoter region, $-928/+21$, $-1738/+21$, $-1979/+21$, and $-2979/+21$ were subject to transcriptional activation by PPAR γ /RXR α , with a maximum of a 4.8-fold increase at 72 h posttransfection. These results predict that the region of the ATGL 5'-flanking sequence that lies 5' to -795 contains *cis* elements that mediate PPAR γ responsiveness. Inspection of the DNA sequence through -2979 of the ATGL 5'-flanking region using DS Gene v1.5 (Accelrys, San Diego, CA) indicates that, although clear PPAR γ /RXR α consensus binding sites are not readily apparent in the promoter region, three PPAR γ half-sites are present at -2424 , -1674 , and -1573 . Even if these are functional sites responsible for transactivation of the $-2979/+21$, $-1979/+21$, and $-1738/+21$ reporter constructs, the responsiveness of the $-928/+21$ construct suggests the possibility that noncanonical PPAR γ binding sites might underlie this response. The exact nature of the DNA elements that mediate the PPAR γ transactivation of ATGL awaits additional analysis of the ATGL promoter; however, the data that we report clearly demonstrate that the ATGL gene is a direct transcriptional target of the key adipo-

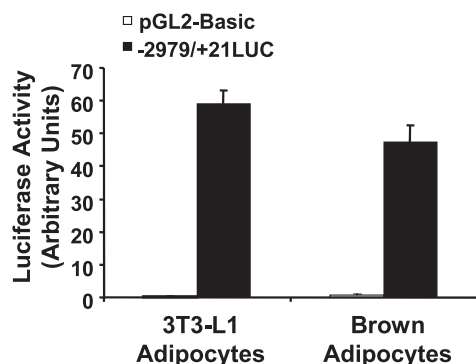


Fig. 8. Promoter activity of ATGL 5'-flanking region in adipocytes. 3T3-L1 adipocytes and brown adipocytes were transfected with the $-2979/+21$ LUC ATGL promoter construct or empty pGL2-Basic vector. After transfection (48 h), cell extracts were harvested for luciferase assay. Firefly luciferase activities were normalized by pRL-TK *Renilla* luciferase activities. Data represent means \pm SD from ≥ 3 independent transfections. Luciferase activities between pGL2-Basic and the $-2979/+21$ LUC construct were determined statistically significant ($P < 0.001$) by single-factor ANOVA.

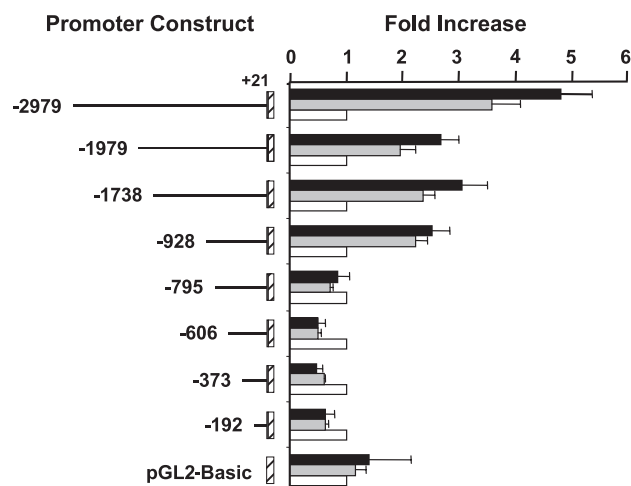


Fig. 9. Transactivation of ATGL 5'-flanking region by PPAR γ . *Left*: schematic diagrams of ATGL luciferase reporter constructs utilized in cotransfection studies. Solid line, ATGL promoter region through +21; hatched box, luciferase reporter gene. Nos. at *left* indicate the 5'-terminal nucleotide of the ATGL 5'-flanking region contained in the corresponding reporter construct. HeLa cells were transfected with indicated promoter constructs in the presence (gray or filled bar) or absence (open bar) of cotransfection with PPAR γ /RXR α . Before harvest (24 h), cells were treated with 10 μ M 15-deoxy- $\Delta^{12,14}$ -prostaglandin J $_2$, a PPAR γ ligand. Gray bar, initial 24-h posttransfection incubation followed by 24 h of ligand treatment with cells harvested 48 h posttransfection; filled bar, initial 48-h posttransfection incubation followed by 24 h of ligand treatment with cells harvested 72 h posttransfection. After ligand incubation, cells were harvested for luciferase assay. Firefly luciferase activities were corrected against the value for cotransfection of pRL-TK *Renilla* luciferase control. *Right*: fold increase in luciferase activities for corresponding ATGL promoter constructs, wherein the value in the absence PPAR γ /RXR α has been normalized to 1. Data represent means \pm SD from a minimum of triplicate transfections, and values in the absence vs. presence of PPAR γ /RXR α were determined statistically significant ($P < 0.001$) by single-factor ANOVA.

cyte transcription factor PPAR γ . Additional studies are planned to determine the precise nature of regulation of the ATGL promoter *in vitro* and *in vivo*.

Characterization of murine ATGL structural gene and comparison with other PNPLA family members. Through phage library screening we identified and analyzed several genomic DNA clones for murine ATGL, and we combined information garnered from these analyses with information present in the Ensembl and NCBI databases to characterize the ATGL gene structure. Murine ATGL is present at the extreme distal arm of chromosome 7 (Fig. 10A), residing between the gene for 60S acidic ribosomal protein P2 (RPLP2) and a gene encoding a novel EF-hand domain protein. The murine ATGL structural gene spans 4.9 kb and comprises 9 exons (Fig. 10B). Examination of the correlation of exon boundaries with corresponding encoded ATGL protein sequences indicates that the patatin domain, which comprises amino acids 10–178 of the ATGL protein and includes the lipase signature motif at amino acids 45–49, is encoded by exons 1–3 and a portion of exon 4. ATGL is one of only five members of the newly recognized PNPLA family of patatin domain-containing proteins. Figure 10C and Table 1 illustrate the relationship among the family members and indicate their respective HUGO nomenclature of PNPLA1–PNPLA5. We are aware of only two additional proteins in the human NCBI Unigene database that possess a patatin domain. These are the calcium-independent phospho-

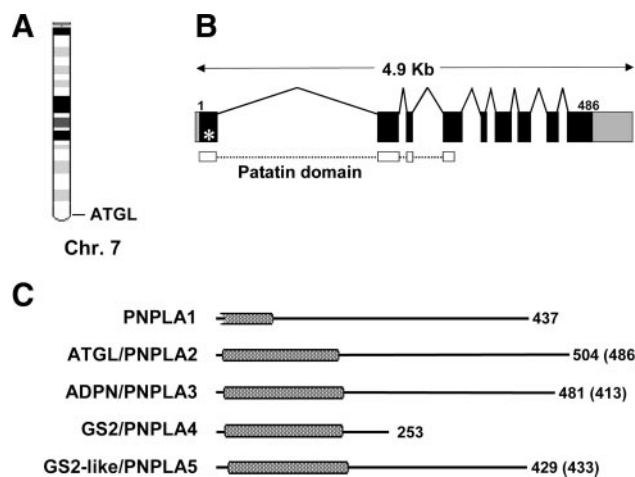


Fig. 10. Intron-exon structure of murine ATGL gene and domain structure of the five PNPLA family proteins. *A*: chromosomal location of murine ATGL. ATGL gene is located on mouse chromosome 7 F5. *B*: gene structure of murine ATGL. ATGL gene contains 9 exons (black box) and 8 introns spanning 4.9 kb. Gray boxes represent 5' and 3' untranslated regions. White boxes and dashed line under the diagram represent patatin domain region; *position of lipase signature motif (GX SXG). *C*: domain relationships among PNPLA family proteins. Shaded rectangular area at left, patatin domain. No. of amino acids for human proteins is shown at right, with no. of amino acids for murine protein following in parentheses.

lipase A₂, group IV, designated PLA2G6, and neuropathy target esterase (NTE), proteins of 806 and 1,327 amino acids, respectively. PLA2G6 is an A₂ phospholipase, a class of enzymes that catalyze the release of fatty acids from phospholipids. The protein has been proposed to function in phospholipid remodeling, release of arachidonic acid, synthesis of prostaglandins, apoptosis, and ion flux in glucose-stimulated β -cells (3, 10, 45, 65). It may also be worthwhile to note that genes for two of the PNPLA family proteins, adiponutrin and GS2-like, as well as for the patatin domain-containing PLA2G6, are each present at human chromosome 22q13.3. NTE catalyzes hydrolysis of membrane lipids and is involved in neuronal development. It is the molecular target for neurodegeneration induced by some organophosphorus pesticides and chemical warfare poisons (32). In contrast to the five PNPLA family proteins wherein the patatin domain is in the NH₂-terminal portion, for PLA2G6 and NTE the patatin domain is positioned in the COOH-terminal half of the protein. In addition, PLA2G6 and NTE possess additional recognizable protein motifs (37). PLA2G6 has multiple ankyrin motifs NH₂-terminal to its patatin domain (65), and NTE has a regulatory domain composed of three CAP effector domain

nucleotide-binding motifs NH₂ terminal to its patatin domain (32). These features serve to distinguish NTE and PLA2G6 from the five PNPLA family proteins.

A picture is emerging that each of the five PNPLA family members might interplay to exert control over triglyceride and FFA homeostasis either in adipocytes or in other cell types via fatty acid turnover and partitioning. ATGL, adiponutrin, GS2, and GS2-like have been demonstrated to possess lipase activity (22, 28, 73, 81). Acyltransferase activity has been demonstrated for ATGL and adiponutrin (22). GS2 (30) was recently reported to possess retinyl ester hydrolase and esterification activities (14). To our knowledge, PNPLA1 has yet to be assessed for enzymatic activities, and the only evidence we are aware of regarding transcript expression of PNPLA1 is via in silico assessments of EST clones. PNPLA1 is present in only one cDNA library, HT1080 cells treated with agents to induce random gene activation (17). In regard to adipose tissue expression, murine ATGL and adiponutrin show marked cell type specificity to adipocytes (4, 22, 28, 73, 81). Human GS2 is expressed in several metabolically active tissues, including adipose (28), and ATGL, adiponutrin, and GS2 are expressed in human SW872 liposarcoma cells (22). Interestingly, assessment of ATGL gene expression in human tissues, as reported by Lake et al. (28), reveals apparent differences with murine expression patterns, with substantial levels of ATGL transcript expression in human adipose tissue, heart, and skeletal muscle, thus emphasizing the necessity to carefully determine the role of the PNPLA proteins in human metabolism and obesity. That PNPLA family proteins may play important roles in energy balance is indicated by their regulation by energy intake level. Murine adiponutrin was identified several years ago as an adipose-specific transcript of unknown function found to be subject to hormonal and dietary regulation (4). However, opposite to ATGL, adiponutrin is dramatically induced during refeeding of mice (4, 28) and rats (47). Studies in humans indicate a moderate increase in adipose tissue adiponutrin transcript upon refeeding (35). A recent study indicated that GS2-like is present as a very-low-abundance transcript in lung and adipose tissue; in the latter case, it is decreased in *ob/ob* adipose tissue and in adipose tissue of fasted mice (28), paralleling that of adiponutrin. In addition to the novel lipases of the PNPLA family, it is not unlikely that adipose tissue expresses additional lipases with a previously unrecognized role in energy balance. For example, Mitchell et al. (61) recently found that adipose tissue expressed carboxylesterase 3, a protein of the endoplasmic reticulum lumen that had been

Table 1. Features of PNPLA family of patatin domain-containing proteins

Designation	Other Names	Chromosome		Function	Adipocyte Expression*	Refs.
		Human	Mouse			
PNPLA1	None	6p21.31	17 A3	Unknown	Unknown	17, 28
PNPLA2	ATGL, Desnutrin, iPLA2 ζ , TTS-2.2	11p15.5	7 F5	TGL, AT, DGGR	Yes	22, 28, 29, 73, 81
PNPLA3	ADPN, iPLA2 ϵ	22q13.31	15 E3	TGL, AT, DGGR	Yes	4, 22, 28, 35, 81
PNPLA4	GS2, iPLA2 η	Xp22.3	ND	TGL, AT, REH, DGGR	Yes	14, 22, 28, 30
PNPLA5	GS2-like	22q13.31	15 E3	DGGR	Yes	28

ATGL, adipose tissue triglyceride lipase; PNPLA1/5, patatin-like phospholipase domain-containing 1/5; iPLA2, calcium-independent phospholipase 2; TGL, triacylglycerol lipase; AT, acyltransferase; REH, retinyl ester hydrolase; DGGR, activity found using 1,2-*o*-dilauryl-rac-glycero-3-glutaric acid-(6'-methyl-resorufin) ester as substrate; ND, not determined. *Transcript expression.

previously implicated in hepatic very low-density lipoprotein synthesis.

In summary, we report that the ATGL transcript is upregulated during multiple models of white and brown adipogenesis and that it is a target for negative regulation by TNF- α and insulin. Furthermore, we have cloned the murine ATGL promoter region and present the first studies on the characterization of the ATGL promoter and report transactivation by the master adipogenic transcriptional regulator PPAR γ . Further studies on the relationship between insulin, TNF- α , and other hormonal signals with ATGL activity and gene expression are needed to determine how transcriptional regulation of ATGL impacts triglyceride balance. In addition, it is possible that, as has been demonstrated for HSL, some degree of posttranscriptional regulation of ATGL activity occurs to coordinately regulate triglyceride hydrolysis. Isoproterenol stimulation results in ATGL phosphorylation, but in contrast to HSL this modification was apparently not mediated by PKA (81). Although appreciation of the full physiological role of ATGL awaits the generation and analysis of the appropriate loss- and gain-of-function *in vivo* models, it is clear that the previously held and relatively straightforward view of triglyceride hydrolysis in adipocytes in normal and in pathophysiological states is in a state of substantial revision. Such reworking should attempt not only to incorporate the recent findings on ATGL but also to better understand the role of the other newly discovered adipose tissue-expressed lipases in the regulation of FFA release from adipocytes.

ACKNOWLEDGMENTS

We thank R. Evans, Salk Institute for Biological Sciences, La Jolla, CA, for the PPAR γ , RXR α , and 3XPPRE-LUC plasmid constructs. RNA for streptozotocin studies was provided by H. S. Sul, University of California, Berkeley, CA. The brown preadipocyte cell line was generously provided by C. R. Kahn, Joslin Diabetes Foundation and Harvard Medical School, Boston, MA. We also thank M. Hammar for excellent technical assistance.

GRANTS

This work was supported in part by National Institute of Diabetes and Digestive and Kidney Diseases Grant 5R21 DK-064992 to C. M. Smas.

REFERENCES

- Andrews DL, Beames B, Summers MD, and Park WD. Characterization of the lipid acyl hydrolase activity of the major potato (*Solanum tuberosum*) tuber protein, patatin, by cloning and abundant expression in a baculovirus vector. *Biochem J* 252: 199–206, 1988.
- Banerji S and Flieger A. Patatin-like proteins: a new family of lipolytic enzymes present in bacteria? *Microbiology* 150: 522–525, 2004.
- Bao S, Jin C, Zhang S, Turk J, Ma Z, and Ramanadham S. Beta-cell calcium-independent group VIA phospholipase A(2) (iPLA(2)beta): tracking iPLA(2)beta movements in response to stimulation with insulin secretagogues in INS-1 cells. *Diabetes* 53, Suppl 1: S186–S189, 2004.
- Baulande S, Lasnier F, Lucas M, and Pairault J. Adiponutrin, a transmembrane protein corresponding to a novel dietary- and obesity-linked mRNA specifically expressed in the adipose lineage. *J Biol Chem* 276: 33336–33344, 2001.
- Botion LM and Green A. Long-term regulation of lipolysis and hormone-sensitive lipase by insulin and glucose. *Diabetes* 48: 1691–1697, 1999.
- Brasaemle DL, Dolios G, Shapiro L, and Wang R. Proteomic analysis of proteins associated with lipid droplets of basal and lipolytically stimulated 3T3-L1 adipocytes. *J Biol Chem* 279: 46835–46842, 2004.
- Brasaemle DL, Levin DM, Adler-Wailles DC, and Londos C. The lipolytic stimulation of 3T3-L1 adipocytes promotes the translocation of hormone-sensitive lipase to the surfaces of lipid storage droplets. *Biochim Biophys Acta* 1483: 251–262, 2000.
- Clifford GM, Londos C, Kraemer FB, Vernon RG, and Yeaman SJ. Translocation of hormone-sensitive lipase and perilipin upon lipolytic stimulation of rat adipocytes. *J Biol Chem* 275: 5011–5015, 2000.
- Cornelius P, Enerback S, Bjursell G, Olivecrona T, and Pekala PH. Regulation of lipoprotein lipase mRNA content in 3T3-L1 cells by tumour necrosis factor. *Biochem J* 249: 765–769, 1988.
- Cummings BS, McHowat J, and Schnellmann RG. Role of an endoplasmic reticulum Ca²⁺-independent phospholipase A2 in cisplatin-induced renal cell apoptosis. *J Pharmacol Exp Ther* 308: 921–928, 2004.
- Egan JJ, Greenberg AS, Chang MK, Wek SA, Moos MC Jr, and Londos C. Mechanism of hormone-stimulated lipolysis in adipocytes: translocation of hormone-sensitive lipase to the lipid storage droplet. *Proc Natl Acad Sci USA* 89: 8537–8541, 1992.
- Fortier M, Wang SP, Mauriege P, Semache M, Mfuma L, Li H, Levy E, Richard D, and Mitchell GA. Hormone-sensitive lipase-independent adipocyte lipolysis during β -adrenergic stimulation, fasting, and dietary fat loading. *Am J Physiol Endocrinol Metab* 287: E282–E288, 2004.
- Fried SK and Zechner R. Cachectin/tumour necrosis factor decreases human adipose tissue lipoprotein lipase mRNA levels, synthesis, and activity. *J Lipid Res* 30: 1917–1923, 1989.
- Gao J and Simon M. Identification of a novel keratinocyte retinyl ester hydrolase as a transacylase and lipase. *J Invest Dermatol* 124: 1259–1266, 2005.
- Haemmerle G, Zimmermann R, Hayn M, Theussl C, Waeg G, Wagner E, Sattler W, Magin TM, Wagner EF, and Zechner R. Hormone-sensitive lipase deficiency in mice causes diglyceride accumulation in adipose tissue, muscle, and testis. *J Biol Chem* 277: 4806–4815, 2002.
- Harada K, Shen WJ, Patel S, Natu V, Wang J, Osuga J, Ishibashi S, and Kraemer FB. Resistance to high-fat diet-induced obesity and altered expression of adipose-specific genes in HSL-deficient mice. *Am J Physiol Endocrinol Metab* 285: E1182–E1195, 2003.
- Harrington JJ, Sherf B, Rundlett S, Jackson PD, Perry R, Cain S, Leventhal C, Thornton M, Ramachandran R, Whittington J, Lerner L, Costanzo D, McElligott K, Boozer S, Mays R, Smith E, Veloso N, Klika A, Hess J, Cothren K, Lo K, Offenbacher J, Danzig J, and Ducar M. Creation of genome-wide protein expression libraries using random activation of gene expression. *Nat Biotechnol* 19: 440–445, 2001.
- Hirschberg HJ, Simons JW, Dekker N, and Egmond MR. Cloning, expression, purification and characterization of patatin, a novel phospholipase A. *Eur J Biochem* 268: 5037–5044, 2001.
- Holm C. Molecular mechanisms regulating hormone-sensitive lipase and lipolysis. *Biochem Soc Trans* 31: 1120–1124, 2003.
- Hotamisligil GS. Molecular mechanisms of insulin resistance and the role of the adipocyte. *Int J Obes Relat Metab Disord* 24, Suppl 4: S23–S27, 2000.
- Huang S, Cerny RE, Bhat DS, and Brown SM. Cloning of an Arabidopsis patatin-like gene, STURDY, by activation T-DNA tagging. *Plant Physiol* 125: 573–584, 2001.
- Jenkins CM, Mancuso DJ, Yan W, Sims HF, Gibson B, and Gross RW. Identification, cloning, expression, and purification of three novel human calcium-independent phospholipase A2 family members possessing triacylglycerol lipase and acylglycerol transacylase activities. *J Biol Chem* 279: 48968–48975, 2004.
- Kim JB and Spiegelman BM. ADD1/SREBP1 promotes adipocyte differentiation and gene expression linked to fatty acid metabolism. *Genes Dev* 10: 1096–1107, 1996.
- Klein J, Fasshauer M, Klein HH, Benito M, and Kahn CR. Novel adipocyte lines from brown fat: a model system for the study of differentiation, energy metabolism, and insulin action. *Bioessays* 24: 382–388, 2002.
- Kralisch S, Klein J, Lossner U, Bluher M, Paschke R, Stumvoll M, and Fasshauer M. Isoproterenol, TNF- α , and insulin downregulate adipose triglyceride lipase in 3T3-L1 adipocytes. *Mol Cell Endocrinol* 240: 43–49, 2005.
- Krey G, Braissant O, L'Horsset F, Kalkhoven E, Perroud M, Parker MG, and Wahli W. Fatty acids, eicosanoids, and hypolipidemic agents identified as ligands of peroxisome proliferator-activated receptors by coactivator-dependent receptor ligand assay. *Mol Endocrinol* 11: 779–791, 1997.
- Laborda J. 36B4 cDNA used as an estradiol-independent mRNA control is the cDNA for human acidic ribosomal phosphoprotein PO. *Nucleic Acids Res* 19: 3998, 1991.
- Lake AC, Sun Y, Li JL, Kim JE, Johnson JW, Li D, Revett T, Shih HH, Liu W, Paulsen JE, and Gimeno RE. Expression, regulation, and

- triglyceride hydrolase activity of Adiponutrin family members. *J Lipid Res* 46: 2477–2487, 2005.
29. **Langin D, Dicker A, Tavernier G, Hoffstedt J, Mairal A, Ryden M, Arner E, Sicard A, Jenkins CM, Viguerie N, van Harmelen V, Gross RW, Holm C, and Arner P.** Adipocyte lipases and defect of lipolysis in human obesity. *Diabetes* 54: 3190–3197, 2005.
 30. **Lee WC, Salido E, and Yen PH.** Isolation of a new gene GS2 (DXS1283E) from a CpG island between STS and KAL1 on Xp22.3. *Genomics* 22: 372–376, 1994.
 31. **Lembertas AV, Perusse L, Chagnon YC, Fiser JS, Warden CH, Purcell-Huynh DA, Dionne FT, Gagnon J, Nadeau A, Lusis AJ, and Bouchard C.** Identification of an obesity quantitative trait locus on mouse chromosome 2 and evidence of linkage to body fat and insulin on the human homologous region 20q. *J Clin Invest* 100: 1240–1247, 1997.
 32. **Li Y, Dinsdale D, and Glynn P.** Protein domains, catalytic activity, and subcellular distribution of neuropathy target esterase in Mammalian cells. *J Biol Chem* 278: 8820–8825, 2003.
 33. **Liang CP and Tall AR.** Transcriptional profiling reveals global defects in energy metabolism, lipoprotein, and bile acid synthesis and transport with reversal by leptin treatment in ob/ob mouse liver. *J Biol Chem* 276: 49066–49076, 2001.
 34. **Liu P, Ying Y, Zhao Y, Mundy DI, Zhu M, and Anderson RG.** Chinese hamster ovary K2 cell lipid droplets appear to be metabolic organelles involved in membrane traffic. *J Biol Chem* 279: 3787–3792, 2004.
 35. **Liu YM, Moldes M, Bastard JP, Bruckert E, Viguerie N, Hainque B, Basdevant A, Langin D, Pairault J, and Clement K.** Adiponutrin: A new gene regulated by energy balance in human adipose tissue. *J Clin Endocrinol Metab* 89: 2684–2689, 2004.
 36. **Lush MJ, Li Y, Read DJ, Willis AC, and Glynn P.** Neuropathy target esterase and a homologous *Drosophila* neurodegeneration-associated mutant protein contain a novel domain conserved from bacteria to man. *Biochem J* 332: 1–4, 1998.
 37. **Marchler-Bauer A, Anderson JB, Cherukuri PF, DeWeese-Scott C, Geer LY, Gwadz M, He S, Hurwitz DI, Jackson JD, Ke Z, Lanczycki CJ, Liebert CA, Liu C, Lu F, Marchler GH, Mullokandov M, Shoemaker BA, Simonyan V, Song JS, Thiessen PA, Yamashita RA, Yin JJ, Zhang D, and Bryant SH.** CDD: a conserved domain database for protein classification. *Nucleic Acids Res* 33: D192–D196, 2005.
 38. **Mignery GA, Pikaard CS, and Park WD.** Molecular characterization of the patatin multigene family of potato. *Gene* 62: 27–44, 1988.
 39. **Moon YS, Latasa MJ, Kim KH, Wang D, and Sul HS.** Two 5'-regions are required for nutritional and insulin regulation of the fatty-acid synthase promoter in transgenic mice. *J Biol Chem* 275: 10121–10127, 2000.
 40. **Mulder H, Sorhede-Winzell M, Contreras JA, Fex M, Strom K, Ploug T, Galbo H, Arner P, Lundberg C, Sundler F, Ahren B, and Holm C.** Hormone-sensitive lipase null mice exhibit signs of impaired insulin sensitivity whereas insulin secretion is intact. *J Biol Chem* 278: 36380–36388, 2003.
 41. **Nardini M and Dijkstra BW.** Alpha/beta hydrolase fold enzymes: the family keeps growing. *Curr Opin Struct Biol* 9: 732–737, 1999.
 42. **Okazaki H, Osuga J, Tamura Y, Yahagi N, Tomita S, Shionoiri F, Iizuka Y, Ohashi K, Harada K, Kimura S, Gotoda T, Shimano H, Yamada N, and Ishibashi S.** Lipolysis in the absence of hormone-sensitive lipase: evidence for a common mechanism regulating distinct lipases. *Diabetes* 51: 3368–3375, 2002.
 43. **Osuga J, Ishibashi S, Oka T, Yagyu H, Tozawa R, Fujimoto A, Shionoiri F, Yahagi N, Kraemer FB, Tsutsumi O, and Yamada N.** Targeted disruption of hormone-sensitive lipase results in male sterility and adipocyte hypertrophy, but not in obesity. *Proc Natl Acad Sci USA* 97: 787–792, 2000.
 44. **Peraldi P, Xu M, and Spiegelman BM.** Thiazolidinediones block tumor necrosis factor- α -induced inhibition of insulin signaling. *J Clin Invest* 100: 1863–1869, 1997.
 45. **Perez R, Melero R, Balboa MA, and Balsinde J.** Role of group VIA calcium-independent phospholipase A2 in arachidonic acid release, phospholipid fatty acid incorporation, and apoptosis in U937 cells responding to hydrogen peroxide. *J Biol Chem* 279: 40385–40391, 2004.
 46. **Plee-Gautier E, Grober J, Duplus E, Langin D, and Forest C.** Inhibition of hormone-sensitive lipase gene expression by cAMP and phorbol esters in 3T3-F442A and BFC-1 adipocytes. *Biochem J* 318: 1057–1063, 1996.
 47. **Polson DA and Thompson MP.** Adiponutrin mRNA expression in white adipose tissue is rapidly induced by meal-feeding a high-sucrose diet. *Biochem Biophys Res Commun* 301: 261–266, 2003.
 48. **Purcell-Huynh DA, Weinreb A, Castellani LW, Mehrabian M, Doolittle MH, and Lusis AJ.** Genetic factors in lipoprotein metabolism. Analysis of a genetic cross between inbred mouse strains NZB/BINJ and SM/J using a complete linkage map approach. *J Clin Invest* 96: 1845–1858, 1995.
 49. **Raben DM and Baldassare JJ.** A new lipase in regulating lipid mobilization: hormone-sensitive lipase is not alone. *Trends Endocrinol Metab* 16: 35–36, 2005.
 50. **Reaven GM.** Banting lecture 1988. Role of insulin resistance in human disease. *Diabetes* 37: 1595–1607, 1988.
 51. **Roduit R, Masiello P, Wang SP, Li H, Mitchell GA, and Prentki M.** A role for hormone-sensitive lipase in glucose-stimulated insulin secretion: a study in hormone-sensitive lipase-deficient mice. *Diabetes* 50: 1970–1975, 2001.
 52. **Rosen ED, Hsu CH, Wang X, Sakai S, Freeman MW, Gonzalez FJ, and Spiegelman BM.** C/EBP α induces adipogenesis through PPAR- γ : a unified pathway. *Genes Dev* 16: 22–26, 2002.
 53. **Rosen ED and Spiegelman BM.** Molecular regulation of adipogenesis. *Annu Rev Cell Dev Biol* 16: 145–171, 2000.
 54. **Rosenbaum SE and Greenberg AS.** The short- and long-term effects of tumor necrosis factor- α and BRL 49653 on peroxisome proliferator-activated receptor (PPAR) γ 2 gene expression and other adipocyte genes. *Mol Endocrinol* 12: 1150–1160, 1998.
 55. **Ruan H, Hacohen N, Golub TR, Van Parijs L, and Lodish HF.** Tumor necrosis factor- α suppresses adipocyte-specific genes and activates expression of preadipocyte genes in 3T3-L1 adipocytes: nuclear factor- κ B activation by TNF- α is obligatory. *Diabetes* 51: 1319–1336, 2002.
 56. **Ruan H and Lodish HF.** Insulin resistance in adipose tissue: direct and indirect effects of tumor necrosis factor- α . *Cytokine Growth Factor Rev* 14: 447–455, 2003.
 57. **Ruan H, Miles PD, Ladd CM, Ross K, Golub TR, Olefsky JM, and Lodish HF.** Profiling gene transcription in vivo reveals adipose tissue as an immediate target of tumor necrosis factor- α : implications for insulin resistance. *Diabetes* 51: 3176–3188, 2002.
 58. **Saltiel AR.** Another hormone-sensitive triglyceride lipase in fat cells? *Proc Natl Acad Sci USA* 97: 535–537, 2000.
 59. **Schrag JD and Cygler M.** Lipases and alpha/beta hydrolase fold. *Methods Enzymol* 284: 85–107, 1997.
 60. **Smih F, Rouet P, Lucas S, Mairal A, Sengenès C, Lafontan M, Vaulont S, Casado M, and Langin D.** Transcriptional regulation of adipocyte hormone-sensitive lipase by glucose. *Diabetes* 51: 293–300, 2002.
 61. **Soni KG, Lehner R, Metalnikov P, O'Donnell P, Semache M, Gao W, Ashman K, Pshezhetsky AV, and Mitchell GA.** Carboxylesterase 3 (EC 3.1.1.1) is a major adipocyte lipase. *J Biol Chem* 279: 40683–40689, 2004.
 62. **Soukas A, Succi ND, Saatkamp BD, Novelli S, and Friedman JM.** Distinct transcriptional profiles of adipogenesis in vivo and in vitro. *J Biol Chem* 276: 34167–34174, 2001.
 63. **Souza SC, Muliro KV, Liscum L, Lien P, Yamamoto MT, Schaffer JE, Dallal GE, Wang X, Kraemer FB, Obin M, and Greenberg AS.** Modulation of hormone-sensitive lipase and protein kinase A-mediated lipolysis by perilipin A in an adenoviral reconstituted system. *J Biol Chem* 277: 8267–8272, 2002.
 64. **Souza SC, Palmer HJ, Kang YH, Yamamoto MT, Muliro KV, Paulson KE, and Greenberg AS.** TNF- α induction of lipolysis is mediated through activation of the extracellular signal related kinase pathway in 3T3-L1 adipocytes. *J Cell Biochem* 89: 1077–1086, 2003.
 65. **Tang J, Kriz RW, Wolfman N, Shaffer M, Seehra J, and Jones SS.** A novel cytosolic calcium-independent phospholipase A2 contains eight ankyrin motifs. *J Biol Chem* 272: 8567–8575, 1997.
 66. **Tansey JT, Sztalryd C, Hlavin EM, Kimmel AR, and Londos C.** The central role of perilipin A in lipid metabolism and adipocyte lipolysis. *IUBMB Life* 56: 379–385, 2004.
 67. **Tontonoz P, Hu E, Graves RA, Budavari AI, and Spiegelman BM.** mPPAR γ 2: tissue-specific regulator of an adipocyte enhancer. *Genes Dev* 8: 1224–1234, 1994.
 68. **Tontonoz P, Hu E, and Spiegelman BM.** Stimulation of adipogenesis in fibroblasts by PPAR γ 2, a lipid-activated transcription factor. *Cell* 79: 1147–1156, 1994.
 69. **Tontonoz P, Kim JB, Graves RA, and Spiegelman BM.** ADD1: a novel helix-loop-helix transcription factor associated with adipocyte determination and differentiation. *Mol Cell Biol* 13: 4753–4759, 1993.

70. **Umlauf E, Csaszar E, Moertelmaier M, Schuetz GJ, Parton RG, and Prohaska R.** Association of stomatin with lipid bodies. *J Biol Chem* 279: 23699–23709, 2004.
71. **Unger RH.** Lipotoxic diseases. *Annu Rev Med* 53: 319–336, 2002.
72. **Unger RH.** Minireview. Weapons of lean body mass destruction: the role of ectopic lipids in the metabolic syndrome. *Endocrinology* 144: 5159–5165, 2003.
73. **Villena JA, Roy S, Sarkadi-Nagy E, Kim KH, and Sul HS.** Desnutrin, an adipocyte gene encoding a novel patatin domain-containing protein, is induced by fasting and glucocorticoids: ectopic expression of desnutrin increases triglyceride hydrolysis. *J Biol Chem* 279: 47066–47075, 2004.
74. **Wang SP, Laurin N, Himms-Hagen J, Rudnicki MA, Levy E, Robert MF, Pan L, Oligny L, and Mitchell GA.** The adipose tissue phenotype of hormone-sensitive lipase deficiency in mice. *Obes Res* 9: 119–128, 2001.
75. **Yeaman SJ.** Hormone-sensitive lipase—new roles for an old enzyme. *Biochem J* 379: 11–22, 2004.
76. **Yu S, Matsusue K, Kashireddy P, Cao WQ, Yeldandi V, Yeldandi AV, Rao MS, Gonzalez FJ, and Reddy JK.** Adipocyte-specific gene expression and adipogenic steatosis in the mouse liver due to peroxisome proliferator-activated receptor gamma1 (PPARgamma1) overexpression. *J Biol Chem* 278: 498–505, 2003.
77. **Zechner R, Newman TC, Sherry B, Cerami A, and Breslow JL.** Recombinant human cachectin/tumor necrosis factor but not interleukin-1 alpha downregulates lipoprotein lipase gene expression at the transcriptional level in mouse 3T3-L1 adipocytes. *Mol Cell Biol* 8: 2394–2401, 1988.
78. **Zechner R, Strauss JG, Haemmerle G, Lass A, and Zimmermann R.** Lipolysis: pathway under construction. *Curr Opin Lipidol* 16: 333–340, 2005.
79. **Zhang B, Berger J, Hu E, Szalkowski D, White-Carrington S, Spiegelman BM, and Moller DE.** Negative regulation of peroxisome proliferator-activated receptor-gamma gene expression contributes to the antiadipogenic effects of tumor necrosis factor-alpha. *Mol Endocrinol* 10: 1457–1466, 1996.
80. **Zimmermann R, Haemmerle G, Wagner EM, Strauss JG, Kratky D, and Zechner R.** Decreased fatty acid esterification compensates for the reduced lipolytic activity in hormone-sensitive lipase-deficient white adipose tissue. *J Lipid Res* 44: 2089–2099, 2003.
81. **Zimmermann R, Strauss JG, Haemmerle G, Schoiswohl G, Birner-Gruenberger R, Riederer M, Lass A, Neuberger G, Eisenhaber F, Hermetter A, and Zechner R.** Fat mobilization in adipose tissue is promoted by adipose triglyceride lipase. *Science* 306: 1383–1386, 2004.

